*Korean J. Chem. Eng.*, **25**(6), 1316-1321 (2008)

# Effect of reaction conditions on the catalytic performance of $Co_9Fe_3Bi_1Mo_{12}O_{51}$ in the oxidative dehydrogenation of n-butene to 1,3-butadiene

**Ji Chul Jung*, Howon Lee*, Sunyoung Park*, Young-Min Chung**, Tae Jin Kim**, Seong Jun Lee**, Seung-Hoon Oh**, Yong Seung Kim**, and In Kyu Song*,†**

*School of Chemical and Biological Engineering, Institute of Chemical Processes, Seoul National University, Shinlim-dong, Gwanak-gu, Seoul 151-744, Korea
**SK Energy Corporation, Yuseong-gu, Daejeon 305-712, Korea
*(Received 29 March 2008 • accepted 21 April 2008)*

**Abstract**–Oxidative dehydrogenation of n-butene to 1,3-butadiene over $Co_9Fe_3Bi_1Mo_{12}O_{51}$ catalyst was conducted in a continuous flow fixed-bed reactor. The effect of reaction conditions (steam/n-butene ratio, reaction temperature, and space velocity) on the catalytic performance of $Co_9Fe_3Bi_1Mo_{12}O_{51}$ was investigated. Steam played an important role in decreasing contact time, suppressing total oxidation of n-butene, and removing coke during the reaction. Yield for 1,3-butadiene showed a volcano-shaped curve with respect to steam/n-butene ratio. The compensation between thermodynamic effect and kinetic effect led to a volcano-shaped curve of 1,3-butadiene yield with respect to reaction temperature. The $Co_9Fe_3Bi_1Mo_{12}O_{51}$ catalyst showed the best catalytic performance at a certain value of space velocity. The optimum steam/n-butene ratio, reaction temperature, and gas hourly space velocity were found to be 15, 420 °C, and 675 $h^{-1}$, respectively.

Key words: Multicomponent Bismuth Molybdate, Reaction Condition, n-Butene, 1,3-Butadiene, Oxidative Dehydrogenation

## INTRODUCTION

1,3-Butadiene is one of the important raw materials in the petrochemical industries [1-3]. It is mostly used for manufacturing styrene-butadiene rubber (SBR), acrylonitrile-butadiene-styrene (ABS) polymer, and polybutadiene rubber (BR) [3,4]. Naphtha cracking is a major process for producing 1,3-butadiene that is currently provided in the market. However, the naphtha cracking process involves many problems in both marketing and energy management, because it produces not only 1,3-butadiene but also many petrochemical raw materials such as ethylene, propylene, and isobutene [5]. Oxidative dehydrogenation of n-butene has attracted much attention as a promising process for producing 1,3-butadiene. The oxidative dehydrogenation of n-butene has many advantages, because this process can be operated as a single unit and is independent of the naphtha cracking unit in producing 1,3-butadiene. Furthermore, no additional major naphtha cracking products are produced in the oxidative dehydrogenation of n-butene [6,7].

A number of catalysts have been investigated for the oxidative dehydrogenation of n-butene, including ferrite-type catalyst [8,9], Cu-Mo catalyst [10], vanadium-containing catalyst [11], and Bi-Mo-based catalyst [12-14]. Among these catalysts, Bi-Mo-based catalysts such as pure bismuth molybdates ($\alpha$-$Bi_2Mo_3O_{12}$, $\beta$-$Bi_2Mo_2O_9$, and $\gamma$-$Bi_2MoO_6$) and multicomponent bismuth molybdates have been extensively studied as efficient catalysts for this reaction [15,16]. In particular, multicomponent bismuth molybdate catalysts have been widely employed to improve the low catalytic activity of pure bismuth molybdate catalysts [17-20].

Multicomponent bismuth molybdate catalysts have the general form of $M^{II}_aM^{III}_bBi_cMo_dO_e$, which includes divalent metal ($M^{II}$), trivalent metal ($M^{III}$), bismuth, and molybdenum [21-23]. Although a number of multicomponent bismuth molybdate catalysts can be formed depending on the constituent metal components and their compositions, it has been reported that $Co_9Fe_3Bi_1Mo_{12}O_{51}$ serves as an efficient multicomponent bismuth molybdate catalyst for the oxidative dehydrogenation of n-butene [24]. In this work, therefore, we chose $Co_9Fe_3Bi_1Mo_{12}O_{51}$ as a model catalyst to investigate the effect of reaction conditions on the catalytic performance of multicomponent bismuth molybdate catalyst in the oxidative dehydrogenation of n-butene.

Steam has been commonly used in the catalytic dehydrogenation reactions such as oxidative dehydrogenation of n-butene. It has been reported that steam serves as a diluent, oxidant, coke remover, and heat sink [25,26]. However, a large amount of steam is not only thermodynamically unfavorable in the oxidative dehydrogenation reaction, but also undesirable in the viewpoint of energy management. Therefore, it is necessary to optimize the amount of steam used in the oxidative dehydrogenation of n-butene.

The oxidative dehydrogenation of n-butene over multicomponent bismuth molybdate catalysts is strongly affected by reaction conditions such as steam/n-butene ratio, reaction temperature, and space velocity. However, not much progress has been made on the effect of reaction conditions on the catalytic performance of multicomponent bismuth molybdate catalyst in the oxidative dehydrogenation of n-butene. Therefore, it would be worthwhile to elucidate the effect of reaction conditions for maximizing the yield for 1,3-butadiene in the oxidative dehydrogenation of n-butene over multicomponent bismuth molybdate.

In this work, a multicomponent bismuth molybdate ($Co_9Fe_3Bi_1Mo_{12}O_{51}$) catalyst was prepared by a co-precipitation method, and was applied to the oxidative dehydrogenation of n-butene to 1,3-

†To whom correspondence should be addressed.
E-mail: inksong@snu.ac.kr

butadiene. The catalyst was characterized by XRD, BET, and ICP-AES analyses. The effect of reaction conditions (steam/n-butene ratio, reaction temperature, and space velocity) on the catalytic performance of $Co_9Fe_3Bi_1Mo_{12}O_{51}$ in the oxidative dehydrogenation of n-butene was investigated.

## EXPERIMENTAL

### 1. Catalyst Preparation

$Co_9Fe_3Bi_1Mo_{12}O_{51}$ catalyst was prepared by a co-precipitation method. 1.5 g of bismuth nitrate ($Bi(NO_3)_3 \cdot 5H_2O$, Sigma-Aldrich) was dissolved in 10 ml of distilled water that had been acidified with 3 ml of concentrated nitric acid. The solution was then added to 100 ml of an aqueous solution containing 7.9 g of cobalt nitrate ($Co(NO_3)_2 \cdot 6H_2O$, Sigma-Aldrich) and 3.7 g of ferric nitrate ($Fe(NO_3)_3 \cdot 9H_2O$, Sigma-Aldrich) to obtain a mixed nitrate solution. The mixed nitrate solution was added dropwise into 50 ml of an aqueous solution containing 6.4 g of ammonium molybdate ($(NH_4)_6Mo_7O_{24} \cdot 4H_2O$, Sigma-Aldrich) under vigorous stirring. After the mixed solution was stirred vigorously at room temperature for 1 h, a solid product was obtained by evaporation. The solid product was dried overnight at 175 °C, and it was then calcined at 475 °C for 5 h in an air stream to yield the $Co_9Fe_3Bi_1Mo_{12}O_{51}$ catalyst.

### 2. Characterization

Formation of $Co_9Fe_3Bi_1Mo_{12}O_{51}$ catalyst was confirmed by XRD (MAC Science, M18XHF-SRA) measurement. Atomic ratio of constituent metal elements was determined by ICP-AES (Shimadz, ICP-1000IV) analysis. Surface area of the catalyst was measured by using a BET apparatus (Micromeritics, ASAP 2010). The amount of carbon deposited on the catalyst surface after the catalytic reaction was measured by CHN elemental analysis (EC Instrument, EA 1110).

### 3. Oxidative Dehydrogenation of n-Butene

Oxidative dehydrogenation of n-butene to 1,3-butadiene over $Co_9Fe_3Bi_1Mo_{12}O_{51}$ catalyst was carried out in a continuous flow fixed-bed reactor in the presence of air and steam, with a variation of steam/n-butene ratio, reaction temperature, and gas hourly space velocity (GHSV). The $Co_9Fe_3Bi_1Mo_{12}O_{51}$ catalyst was pretreated at 470 °C for 1 h with an air stream (16 ml/min). Water was sufficiently vaporized by passing through a pre-heating zone and was continuously fed into the reactor together with n-butene and air. $C_4$ raffinate-3 containing 57.9 wt% n-butene (1-butene (7.5 wt%)+trans-2-butene (33.9 wt%)+cis-2-butene (16.5 wt%)) was used as a n-butene source, and air was used as an oxygen source (nitrogen in air served as a carrier gas). $C_4$ raffinate-3 was composed of 57.9 wt% n-butene, 41.6 wt% n-butane, 0.3 wt% cyclobutane, 0.1 wt% methyl cyclopropane, and 0.1 wt% residue. Reaction products were periodically sampled and analyzed by gas chromatograph. Conversion of n-butene and selectivity for 1,3-butadiene were calculated on the basis of carbon balance as follows. Yield for 1,3-butadiene was calculated by multiplying conversion and selectivity.

$$\text{Conversion of n-butene} = \frac{\text{moles of n-butene reacted}}{\text{moles of n-butene supplied}} \quad (1)$$

$$\text{Selectivity for 1,3-butadiene} = \frac{\text{moles of 1,3-butadiene formed}}{\text{moles of n-butene reacted}} \quad (2)$$

## RESULTS AND DISCUSSION

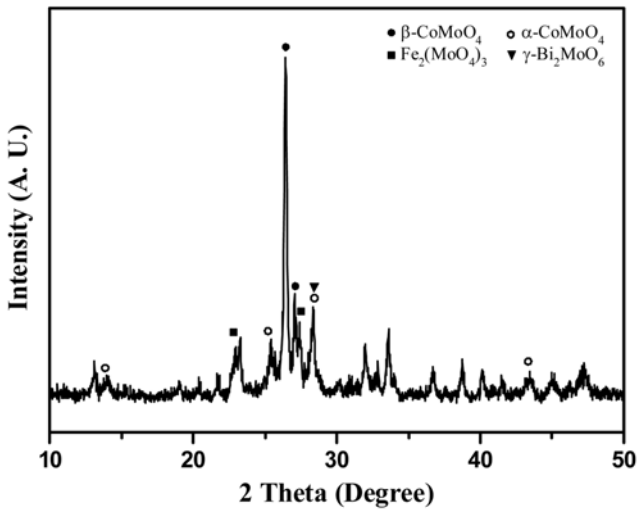


**Fig. 1. XRD pattern of $Co_9Fe_3Bi_1Mo_{12}O_{51}$ catalyst.**

### 1. Formation and Characterization of $Co_9Fe_3Bi_1Mo_{12}O_{51}$ Catalyst

Successful formation of $Co_9Fe_3Bi_1Mo_{12}O_{51}$ catalyst was confirmed by XRD measurement. Fig. 1 shows the XRD pattern of $Co_9Fe_3Bi_1Mo_{12}O_{51}$ catalyst. Each phase was identified by its characteristic diffraction peaks by using JCPDS. It was found that the $Co_9Fe_3Bi_1Mo_{12}O_{51}$ catalyst was composed of four major mixed phases of $\beta$-$CoMoO_4$, $\alpha$-$CoMoO_4$, $Fe_2(MoO_4)_3$, and $\gamma$-$Bi_2MoO_6$. This result was well consistent with a previous report [17], indicating successful formation of $Co_9Fe_3Bi_1Mo_{12}O_{51}$ catalyst. Atomic ratio of constituent metal components determined by ICP-AES analysis was found to be Co : Fe : Bi : Mo=9.0 : 3.2 : 1.0 : 11.4, in good agreement with the theoretical value. This result also indicates that $Co_9Fe_3Bi_1Mo_{12}O_{51}$ catalyst was successfully prepared in this work. BET surface area of the catalyst was found to be very low (2.3 $m^2/g$), as reported in the previous work [17].

Although a number of structural models for multicomponent bismuth molybdate catalysts have been suggested, many researchers agree that a particle model proposed by Wolfs et al. is largely acceptable [18,27]. Fig. 2 shows the particle model for Co-Fe-Bi-

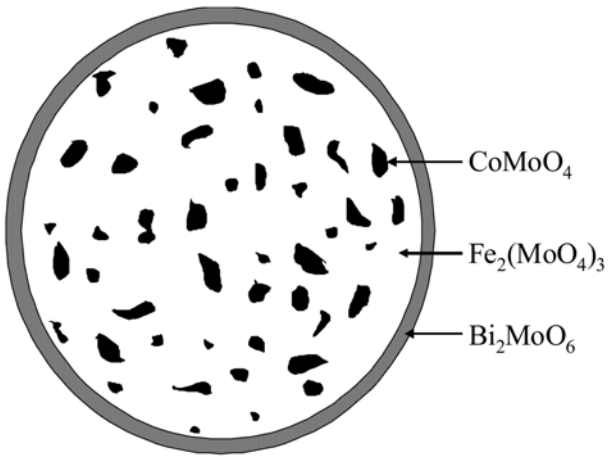


**Fig. 2. Particle model for Co-Fe-Bi-Mo-O catalyst.**

Mo-O catalyst. According to this model, a multicomponent bismuth molybdate catalyst consists of a core of divalent and trivalent metal molybdates with a thin shell of bismuth molybdate. The bismuth molybdate located on the surface of the catalyst serves as an active phase, while the divalent and trivalent metal molybdates concentrated in the bulk of the catalyst act as a support for the active component in the multicomponent bismuth molybdate catalyst system [17]. The divalent and trivalent metal molybdates in the bulk of the catalyst facilitate the migration of active oxygen species to the bismuth molybdate on the catalyst surface, leading to an enhanced oxygen mobility of multicomponent bismuth molybdate catalyst [19].

It is generally accepted that the oxidative dehydrogenation of n-butene to 1,3-butadiene follows the Mars-van Krevelen mechanism [28,29]. According to this mechanism, oxygen in the catalyst directly reacts with n-butene, and in turn, oxygen in the gas phase makes up oxygen vacancy in the catalyst. This means that oxygen mobility of the catalyst plays an important role in determining the catalytic performance in the oxidative dehydrogenation of n-butene. When compared to the pure bismuth molybdate catalysts, the high catalytic activity of multicomponent bismuth molybdate catalysts in the oxidative dehydrogenation of n-butene is believed to be due to their facile oxygen mobility [17,24].

**2. Effect of Steam**

The role and effect of steam on the catalytic performance of $Co_9Fe_3Bi_1Mo_{12}O_{51}$ in the oxidative dehydrogenation of n-butene was investigated. For this purpose, a catalytic reaction was carried out at 420 °C with a variation of steam/n-butene ratio (n-butene : oxygen : steam=1 : 0.75 : 5-30). Based on our preliminary experiments, the ratio of n-butene : oxygen was fixed at 1 : 0.75. GHSV was fixed at 475 $h^{-1}$ on the basis of n-butene. Fig. 3 shows the catalytic performance of $Co_9Fe_3Bi_1Mo_{12}O_{51}$ in the oxidative dehydrogenation of n-butene at 420 °C after a 6 h-reaction, plotted as a function of steam/n-butene ratio. In the catalytic reaction, $CO_2$ was mainly produced as a by-product and CO formation was negligible.

As shown in Fig. 3, conversion of n-butene and yield for 1,3-butadiene showed volcano-shaped curves with respect to steam/n-butene ratio. The maximum conversion of n-butene (66.8%) and the maximum yield for 1,3-butadiene (60.6%) were observed at a steam/n-butene ratio of 15. It is interesting to note that selectivity for 1,3-butadiene slightly increased with increasing steam/n-butene ratio, while selectivity for $CO_2$ decreased with increasing steam/n-butene ratio. This indicates that steam played an important role in suppressing total oxidation of n-butene in the oxidative dehydrogenation of n-butene.

Although steam is widely used as a diluent, oxidant, coke remover, and heat sink in the partial oxidation of hydrocarbons, the role of steam is still controversial. It has been reported that steam enhanced the catalytic activity of magnesium ferrites in the oxidative dehydrogenation of n-butene [25]. This promotion effect of steam was attributed to the hydroxylation of the catalyst surface. Steam also served as a diluent in the reaction, leading to an increment of total flow rate. The increase of total flow rate (the decrease of contact time) gave rise to the decrease of n-butene conversion in the oxidative dehydrogenation of n-butene. It has also been reported that steam shows two compensating effects in the oxidative dehydrogenation of n-butene over iron oxide catalyst [30]; one effect is to increase the activity by converting the catalyst surface into a hydroxyl form, and the other effect is to suppress the activity by causing competitive adsorption of molecular water on the catalyst surface. Saleh-Alhamed et al. have suggested that steam played the following two roles in the oxidation of propylene over multicomponent metal oxide catalysts: blockage of total oxidation sites and creation of new active sites for partial oxidation [31,32].

From the fact that conversion of n-butene and yield for 1,3-butadiene showed volcano-shaped curves with respect to steam/n-butene ratio, it can be inferred that steam also played two compensating roles in our catalytic reaction system. It is reasonable to expect that steam served as a diluent in the reaction, leading to a lower conversion of n-butene with increasing steam/n-butene ratio. However, the positive effect of steam enhancing the conversion of n-butene with increasing steam/n-butene ratio has not been clearly determined yet.

As mentioned earlier, $CO_2$ formation was suppressed by the addition of steam to the feed in the oxidative dehydrogenation of n-butene over $Co_9Fe_3Bi_1Mo_{12}O_{51}$ catalyst. This indicates that steam played an important role in suppressing total oxidation of n-butene to $CO_2$ by blocking total oxidation sites of $Co_9Fe_3Bi_1Mo_{12}O_{51}$ cata-

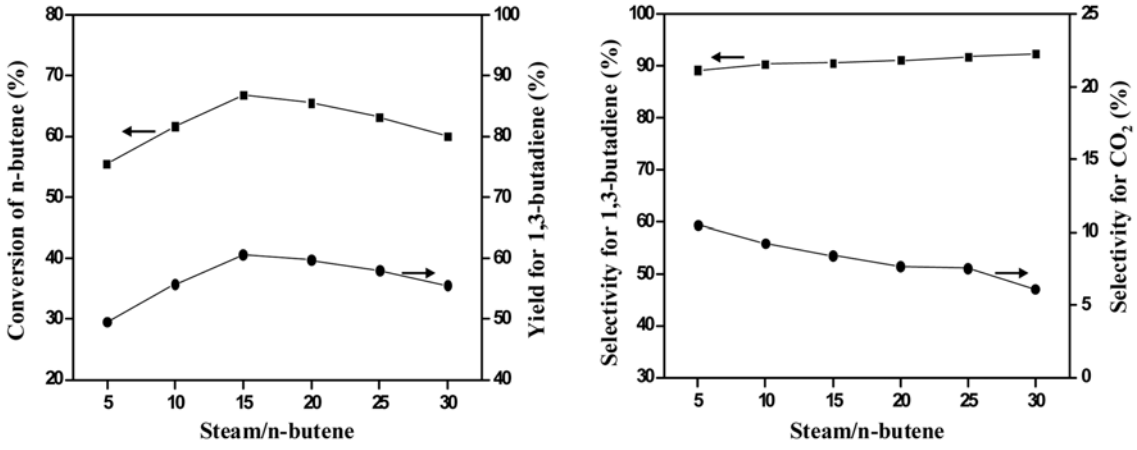


**Fig. 3. Catalytic performance of $Co_9Fe_3Bi_1Mo_{12}O_{51}$ in the oxidative dehydrogenation of n-butene after a 6 h-reaction, plotted as a function of steam/n-butene ratio: reaction temperature=420 °C, GHSV=475 $h^{-1}$.**

**Table 1. Amount of carbon deposited on the catalyst surface with a variation of steam/n-butene ratio after a 6 h-reaction**

| Steam/n-butene | 5 | 10 | 15 | 20 | 25 | 30 |
|---|---|---|---|---|---|---|
| Carbon (wt%) | 0.41 | 0.36 | 0.27 | 0.20 | 0.15 | 0.13 |

lyst. This result is in good agreement with previous reports [31-33]. In our catalytic reaction, the decrease in $CO_2$ selectivity is equivalent to the increase in 1,3-butadiene selectivity, leading to an enhanced selectivity for 1,3-butadiene with increasing steam/n-butene ratio.

In order to confirm the role of steam in removing coke, the amount of carbon deposited on the catalyst surface after a 6 h-reaction was measured by CHN elemental analysis. The amount of carbon deposited on the catalyst surface with a variation of steam/n-butene ratio is summarized in Table 1. The amount of carbon decreased with increasing steam/n-butene ratio. This indicates that steam played an important role in removing coke deposited on the catalyst surface during the oxidative dehydrogenation of n-butene.

It can be summarized that steam played an essential role in decreasing contact time, suppressing total oxidation of n-butene, and removing coke deposited during the reaction. In addition, steam served as a heat sink for preventing hot spots or reactor run-away and played a role in regenerating active sites of the catalyst [32].

### 3. Effect of Reaction Temperature

The effect of reaction temperature on the catalytic performance of $Co_9Fe_3Bi_1Mo_{12}O_{51}$ was investigated by carrying out the catalytic reaction at temperatures ranging from 380 to 460 °C. Feed composition of n-butene:oxygen:steam was fixed at 1 : 0.75 : 15, because the maximum yield for 1,3-butadiene was observed at steam/n-butene ratio of 15 (Fig. 3). GHSV was fixed at 475 $h^{-1}$ on the basis of n-butene. Fig. 4 shows the catalytic performance of $Co_9Fe_3Bi_1Mo_{12}O_{51}$ in the oxidative dehydrogenation of n-butene after a 6 h-reaction, plotted as a function of reaction temperature. Conversion of n-butene and yield for 1,3-butadiene showed volcano-shaped curves with respect to reaction temperature. In particular, conversion of n-butene and yield for 1,3-butadiene were slightly increased with increasing reaction temperature within the range of 380-420 °C, but were drastically decreased with increasing reaction temperature above 420 °C.

As mentioned earlier, multicomponent bismuth molybdate catalyst is composed of mixed phases of various metal molybdates such as divalent metal molybdate, trivalent metal molybdate, and bismuth molybdate. These metal molybdates can also have different phases such as $\alpha$- and $\beta$-metal molybdates depending on reaction temperature [34-37]. This implies that any phase transformation in the catalyst may occur during the catalytic reaction. In order to check

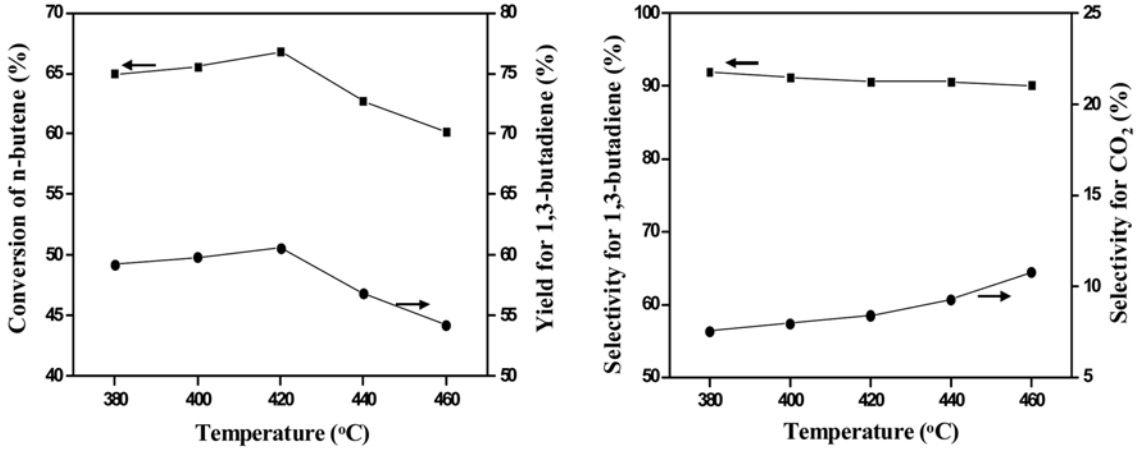


**Fig. 4. Catalytic performance of $Co_9Fe_3Bi_1Mo_{12}O_{51}$ in the oxidative dehydrogenation of n-butene after a 6 h-reaction, plotted as a function of reaction temperature: n-butene : oxygen : steam=1 : 0.75 : 15, GHSV=475 $h^{-1}$.**

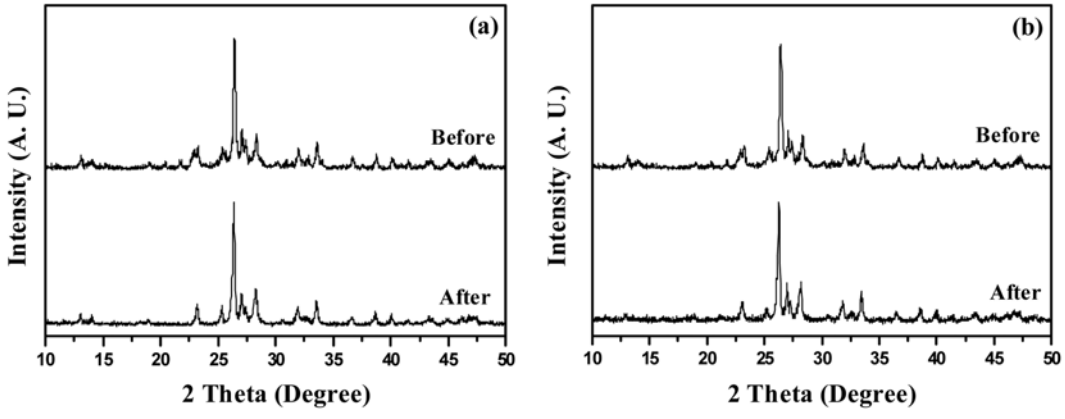


**Fig. 5. XRD patterns of $Co_9Fe_3Bi_1Mo_{12}O_{51}$ catalyst obtained before and after a 6 h-reaction at (a) 420 and (b) 460 °C.**

measurements were conducted before and after the reaction. Fig. 5 shows the XRD patterns of $Co_9Fe_3Bi_1Mo_{12}O_{51}$ obtained before and after a 6 h-reaction at 420 and 460 °C. It is noteworthy that the $Co_9Fe_3Bi_1Mo_{12}O_{51}$ catalyst showed no noticeable difference in XRD patterns before and after the reaction performed at 420 and 460 °C. No difference in XRD patterns before and after the reaction was also observed at the reaction temperature of 380-420 °C (although these are not shown here). The above result indicates that the $Co_9Fe_3Bi_1Mo_{12}O_{51}$ catalyst was thermally stable during the catalytic reaction performed at 380-420 °C. In other words, the result means that the decrement in 1,3-butadiene yield at the reaction temperature above 420 °C was not due to any phase transformation in the $Co_9Fe_3Bi_1Mo_{12}O_{51}$ catalyst.

It is known that the oxidative dehydrogenation of n-butene to 1,3-butadiene is an exothermic reaction, indicating that the increase of reaction temperature is thermodynamically unfavorable [5,33]. From the viewpoint of kinetics, however, the oxidative dehydrogenation of n-butene is promoted with increasing reaction temperature. When considering that conversion of n-butene showed a volcano-shaped curve with respect to reaction temperature, it is believed that the oxidative dehydrogenation of n-butene over $Co_9Fe_3Bi_1Mo_{12}O_{51}$ catalyst was simultaneously influenced by thermodynamics and kinetics. Thus, the compensation between thermodynamic effect and kinetic effect led to a volcano-shaped curve of 1,3-butadiene yield with respect to reaction temperature.

As shown in Fig. 4, selectivity for 1,3-butadiene decreased with increasing reaction temperature, while selectivity for $CO_2$ increased with increasing reaction temperature. This indicates that a higher reaction temperature was not always favorable in the oxidative dehydrogenation of n-butene to 1,3-butadiene.

**4. Effect of GHSV**

In order to investigate the effect of GHSV on the catalytic performance of $Co_9Fe_3Bi_1Mo_{12}O_{51}$ in the oxidative dehydrogenation of n-butene, a catalytic reaction was performed with a variation of GHSV (275-1,275 $h^{-1}$). GHSV was calculated on the basis of n-butene feed. The reaction temperature and n-butene : oxygen : steam composition were fixed at 420 °C and 1 : 0.75 : 15, respectively. Fig. 6 shows the catalytic performance of $Co_9Fe_3Bi_1Mo_{12}O_{51}$ in the oxidative dehydrogenation of n-butene after a 6 h-reaction, plotted as a function of GHSV. Conversion of n-butene decreased with increasing GHSV. This is not surprising, because an increment in GHSV decreases the contact time, leading to a lower conversion of n-butene. What is interesting is that selectivity for 1,3-butadiene increased with increasing GHSV, while selectivity for $CO_2$ decreased with increasing GHSV. Yield for 1,3-butadiene showed high values at low GHSVs. The maximum yield for 1,3-butadiene was obtained at 675 $h^{-1}$ (61.3%).

## CONCLUSIONS

$Co_9Fe_3Bi_1Mo_{12}O_{51}$ catalyst was prepared by a co-precipitation method, and was applied to the oxidative dehydrogenation of n-butene to 1,3-butadiene in a continuous flow fixed-bed reactor. The effect of reaction conditions (steam/n-butene ratio, reaction temperature, and GHSV) on the catalytic performance of $Co_9Fe_3Bi_1Mo_{12}O_{51}$ in the oxidative dehydrogenation of n-butene was investigated. Yield for 1,3-butadiene showed volcano-shaped curves with respect to steam/n-butene ratio and reaction temperature. On the other hand, yield for 1,3-butadiene showed high values at low GHSVs. Steam played an important role in decreasing contact time, suppressing total oxidation of n-butene to $CO_2$, and removing coke deposited during the reaction. The compensation between thermodynamic effect and kinetic effect led to a volcano-shaped curve of 1,3-butadiene yield with respect to reaction temperature. The $Co_9Fe_3Bi_1Mo_{12}O_{51}$ catalyst showed the best catalytic performance at a certain value of GHSV. The maximum yield for 1,3-butadiene (61.3%) over $Co_9Fe_3Bi_1Mo_{12}O_{51}$ catalyst was obtained at the reaction conditions of steam/n-butene ratio of 15, reaction temperature of 420 °C, and GHSV of 675 $h^{-1}$.

## ACKNOWLEDGMENTS

The authors wish to acknowledge support from the Korea Energy Management Corporation (2005-01-0090-3-010).

## REFERENCES

1. S. C. Oh, H. P. Lee, H. T. Kim and K. O. Yoo, *Korean J. Chem. Eng.*,

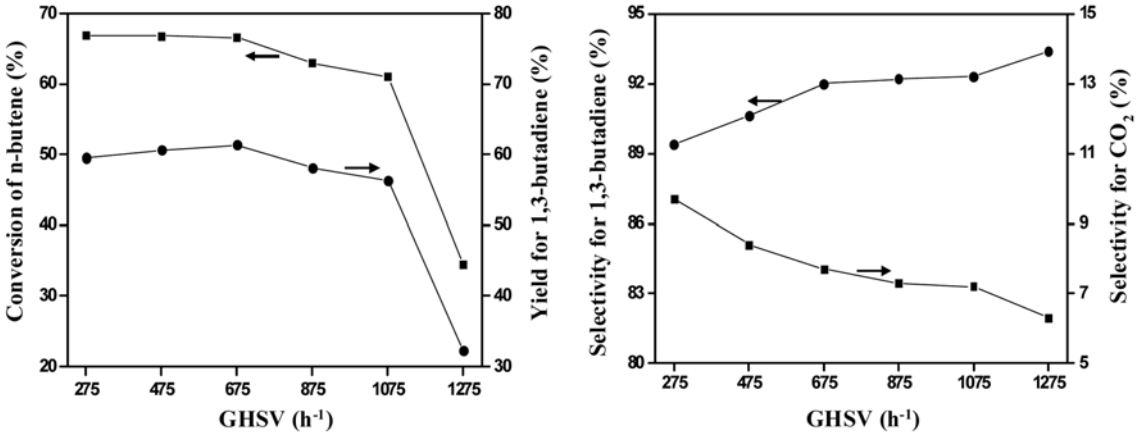


**Fig. 6. Catalytic performance of $Co_9Fe_3Bi_1Mo_{12}O_{51}$ in the oxidative dehydrogenation of n-butene after a 6 h-reaction, plotted as a function of GHSV: n-butene : oxygen : steam=1 : 0.75 : 15, reaction temperature=420 °C.**

**16**, 543 (1999).
2. Ph. A. Batist, J. F. H. Bouwens and G. C. A. Schuit, *J. Catal.*, **25**, 1 (1972).
3. R. K. Grasselli, *Topics Catal.*, **21**, 79 (2002).
4. W. J. Linn and A. W. Sleight, *J. Catal.*, **41**, 134 (1976).
5. L. M. Madeira and M. F. Portela, *Catal. Rev.*, **44**, 247 (2002).
6. A. P. V. Soares, L. D. Dimitrov, M. C. A. Oliveira, L. Hilaire, M. F. Portela and R. K. Grasselli, *Appl. Catal. A*, **253**, 191 (2003).
7. H. H. Kung, *Adv. Catal.*, **40**, 1 (1994).
8. H. Lee, J. C. Jung, H. Kim, Y.-M. Chung, T. J. Kim, S. J. Lee, S.-H. Oh, Y. S. Kim and I. K. Song, *Catal. Commun.*, **9**, 1137 (2008).
9. J. M. López Nieto, P. Concepción, A. Dejoz, H. Knözinger, F. Melo and M. I. Vázquez, *J. Catal.*, **189**, 147 (2000).
10. P. N. Tiwari, T. G. Alkhazov, K. U. Adzamov and A. K. Khanmamedova, *J. Catal.*, **120**, 278 (1989).
11. J. A. Toledo-Antonio, N. Nava, M. Matínez and X. Bokhimi, *Appl. Catal. A*, **234**, 137 (2002).
12. D. A. G. van Oeffelen, J. H. C. van Hooff and G. C. A. Schuit, *J. Catal.*, **95**, 84 (1985).
13. M. Egashira, K. Matsuo, S. Kagawa and T. Seiyama, *J. Catal.*, **58**, 409 (1979).
14. Ph. A. Batist, B. C. Lippens and G. C. A. Schuit, *J. Catal.*, **5**, 55 (1966).
15. J. C. Jung, H. Kim, A. S. Choi, Y.-M. Chung, T. J. Kim, S. J. Lee, S.-H. Oh and I. K. Song, *J. Mol. Catal. A*, **259**, 166 (2006).
16. E. V. Hoefs, J. R. Monnier and G. W. Keulks, *J. Catal.*, **57**, 331 (1979).
17. Y. Moro-oka and W. Ueda, *Adv. Catal.*, **40**, 233 (1994).
18. M. W. J. Wolfs and Ph. A. Batist, *J. Catal.*, **32**, 25 (1974).
19. D.-H. He, W. Ueda and Y. Moro-oka, *Catal. Lett.*, **12**, 35 (1992).
20. W. Ueda, K. Asakawa, C.-L. Chen, Y. Moro-oka and T. Ikawa, *J. Catal.*, **101**, 360 (1986).
21. C. F. Cullis and D. J. Hucknall, *A specialist periodical report: Catalysis*, Royal Chem. Soc., London (1982).
22. R. K. Grasselli and J. D. Burrington, *Adv. Catal.*, **30**, 133 (1981).
23. H. H. Kung and M. C. Kung, *Adv. Catal.*, **33**, 159 (1985).
24. J. C. Jung, H. Lee, H. Kim, Y.-M. Chung, T. J. Kim, S. J. Lee, S.-H. Oh, Y. S. Kim and I. K. Song, *Catal. Commun.*, **9**, 447 (2008).
25. B. L. Yang, D. S. Cheng and S. B. Lee, *Appl. Catal.*, **70**, 161 (1991).
26. E. H. Lee, *Catal. Rev.*, **8**, 285 (1973).
27. I. Matsuura and M. W. J. Wolfs, *J. Catal.*, **37**, 174 (1975).
28. M. F. Porteal, *Topics Catal.*, **15**, 241 (2001).
29. R. K. Grasselli, *Handbook of heterogeneous catalysis*, Wiley, New York (1997).
30. B. J. Liaw, D. S. Cheng and B. L. Yang, *J. Catal.*, **118**, 312 (1989).
31. Y. A. Saleh-Alhamed, R. R. Hudgins and P. L. Silvestion, *J. Catal.*, **161**, 430 (1996).
32. Y. A. Saleh-Alhamed, R. R. Hudgins and P. L. Silvestion, *Appl. Catal. A*, **127**, 177 (1995).
33. J. C. Jung, H. Kim, Y. S. Kim, Y.-M. Chung, T. J. Kim, S. J. Lee, S.-H. Oh and I. K. Song, *Appl. Catal. A*, **317**, 244 (2007).
34. J. A. Rodriguez, S. Chaturvedi, J. C. Hanson, A. Albornoz and J. L. Brito, *J. Phys. Chem. B*, **102**, 1347 (1998).
35. K. H. Lee, Y.-S. Yoon, W. Ueda and Y. Moro-oka, *Catal. Lett.*, **46**, 267 (1997).
36. J. A. Rodriguez, J. C. Hanson, S. Chaturvedi, A. Maiti and J. L. Brito, *J. Chem. Phys.*, **112**, 935 (2000).
37. J. L. Brito and A. L. Barbosa, *J. Catal.*, **171**, 467 (1997).